### RESEARCH ARTICLE

## Transient ammonia stress on Chinese hamster ovary (CHO) cells yield alterations to alanine metabolism and IgG glycosylation profiles

Benjamin F. Synoground<sup>1</sup> | Claire E. McGraw<sup>2</sup> | Kathryn S. Elliott<sup>1</sup> | Christina Leuze<sup>1,3</sup> | Jada R. Roth<sup>2</sup> | Sarah W. Harcum<sup>1</sup> | Nicholas R. Sandoval<sup>2</sup> •

#### Correspondence

Nicholas R. Sandoval, Department of Chemical and Biomolecular Engineering, Tulane University, New Orleans, Louisiana, USA. Email: nsandova@tulane.edu

Benjamin F. Synoground and Claire E. McGraw contributed equally.

#### Abstract

Background: Ammonia concentrations typically increase during mammalian cell cultures, mainly due to glutamine and other amino acid consumption. An early ammonia stress indicator is a metabolic shift with respect to alanine. To determine the underlying mechanisms of this metabolic shift, a Chinese hamster ovary (CHO) cell line with two distinct ages (standard and young) was cultured in parallel fed-batch bioreactors with 0 mM or 10 mM ammonia added at 12 h. Reduced viable cell densities were observed for the stressed cells, while viability was not significantly affected. The stressed cultures had higher alanine, lactate, and glutamate accumulation. Interestingly, the ammonia concentrations were similar by Day 8.5 for all cultures. We hypothesized the ammonia was converted to alanine as a coping mechanism. Interestingly, no significant differences were observed for metabolite profiles due to cell age. Glycosylation analysis showed the ammonia stress reduced galactosylation, sialylation, and fucosylation. Transcriptome analysis of the standard-aged cultures indicated the ammonia stress had a limited impact on the transcriptome, where few of the significant changes were directly related metabolite or glycosylation reactions. These results indicate that mechanisms used to alleviate ammonia stress are most likely controlled post-transcriptionally, and this is where future research should focus.

#### **KEYWORDS**

alanine metabolism, ambr250, ammonia stress, Chinese hamster ovary cells, ribosome genes

Abbreviations:  $\alpha$ KG,  $\alpha$ -ketoglutarate; ALT, alanine transaminase; CE-HPMS, capillary electrophoresis with high pressure mass spectrometry; CHO, Chinese hamster ovary; COA, critical quality attribute; DB, deadband; DO, dissolved oxygen; FC, Fold change; FDR, false discovery rate; GC-FID, gas chromatography-flame ionization detector; GDH, glutamate dehydrogenase; GLM, generalized linear model;  $K_m$ , Michaelis-Menten constant;  $IgG_1$ , immunoglobulin G1; IVCD, integral viable cell density; LRT, likelihood ratio test; NCBI, National Center for Biotechnology Information; NIH, National Institutes of Health: PCA. principal component analysis; PDL, population doubling level; PBS, phosphate-buffered saline; pHi. intracellular pH: PID, proportion-integral-differential: RIN, RNA integrity number: RNA-Seq, RNA sequencing; SD, standard deviation; SRA, Sequence Read Archive; TCA, tricarboxylic acid cycle; UPLC, ultra-performance liquid chromatography; VCD, viable cell density; v/v, volume per volume

## 1 | INTRODUCTION

Ammonia is a well-recognized toxic and inhibitory by-product of amino acid catabolism primarily produced in the mitochondria.[1-4] During high-cell density fed-batch cultures it is common to reach viable cell densities (VCD) up to 50 million cells per mL with ammonia levels gradually increasing to values between 10 and 20 mM.<sup>[5,6]</sup> Process intensification has substantially increased challenges surrounding ammonia and similar waste product accumulation for Chinese hamster ovary (CHO) cell cultures, as waste product species are

<sup>&</sup>lt;sup>1</sup> Department of Bioengineering, Clemson University, Clemson, South Carolina, USA

<sup>&</sup>lt;sup>2</sup> Department of Chemical and Biomolecular Engineering, Tulane University, New Orleans, Louisiana, USA

<sup>&</sup>lt;sup>3</sup> Department of Molecular Biotechnology, Heidelberg University, Heidelberg, Germany

known to be growth and product inhibitors.  $^{[2,7-9]}$  And recent work has demonstrated that ammonia stress can induce microsatellite instability, in a dose-dependent manner.  $^{[10]}$  Specifically, elevated ammonia levels have been observed to inhibit cell growth and maximum cell densities, decrease titer production, and negatively affect critical quality attributes (CQA).  $^{[6,11,12]}$ 

Several mechanisms of ammonia toxicity have been proposed with the majority originating from the intracellular pH (pH<sub>i</sub>) changes. [6.11,13-15] Normal bioprocess pH setpoints range from 6.9 – 7.3. In this range, nearly all the ammonia exists in its ionized form, NH<sub>4</sub>+, and the concentration of dissolved NH<sub>3</sub> is very low (pK<sub>a</sub> = 9.2). [16] The ionized form is relatively membrane impermeable and competes with potassium ions for uptake due to similar ionic radii. [17-19] Subsequently, intracellular K+ concentrations decrease and maintenance energy requirements increase to maintain ion gradients. [20-22] The addition of NH<sub>4</sub>Cl acidifies the cytoplasm and results in slight alkalinization of the mitochondria. [22] Even though the alkaline environment in the mitochondria is thought to have nominal effects on the proton gradient, others have pointed out that many key central metabolic enzymes are highly pH-dependent. [16,21,23-27]

Academic and industrial research groups have spent over 30 years developing methods to minimize ammonia and waste product accumulation with better progress made reducing lactate than ammonia accumulation.<sup>[9,28-32]</sup> Most commonly, exogenous ammonia is utilized to simulate ammonia stress to disconnect the metabolic effects.<sup>[6,7,12,33]</sup> Yet, the basic rules of thumb to minimize ammonia accumulation are to use alternative carbon and nitrogen sources and improve process control of the carbon/nitrogen concentrations.<sup>[7,30,34-36]</sup> Genetic engineering approaches have also been used to minimize ammonia accumulation or decrease toxicity on the cells.<sup>[37-41]</sup> Nonetheless, the literature reports are mixed with respect to the degree these interventions are successful.<sup>[2,28]</sup>

To gain a better understanding of the effects ammonia has on cellular metabolism and other interactions, several researchers have investigated gene expression in CHO cells in response to ammonia stress. [12,33,42] Early studies identified a few genes involved in glycosylation that were down-regulated; [12] and once the CHO genome was sequenced, it was determined that other glycosylation-related genes were also negatively impacted by elevated ammonia; [33] however, a whole genome examination has not been undertaken. In the interim, researchers have disrupted amino acid pathways in CHO cells to reduce ammonia accumulation. [38,43] There is evidence of strong metabolic correlation between ammonia stress and amino acid metabolism, specifically alanine biosynthesis. It is unknown if metabolic enzyme gene expressions change in response to elevated ammonia to enhance detoxification reactions. [44]

In this study, parallel fed-batch CHO cell cultures of two distinct ages were treated with either a 10 mM ammonia stress with bolus addition of NH $_4$ Cl or an equal basal media bolus in an ambr250 system. The two-level factorial design was selected to simulate common end of culture ammonia concentrations and evaluate the age-dependent stress response to ammonia. Growth, metabolite, and glycosylation profiles were compared across both young- and standard-aged cultures. Addi-

tionally, both transcriptomic and amino acid metabolic analyses were conducted on the standard-aged cultures to determine the underlying cellular mechanisms for the observed differences in bioprocess and growth profiles, specific metabolite production rates, and CQA.

## 2 | MATERIALS AND METHODS

#### 2.1 | Cell culture

Recombinant CHO-K1 Clone A11 expressing the anti-HIV antibody VRC01 ( $IgG_1$ ) was obtained from the Vaccine Research Center at the National Institutes of Health (NIH). The CHO VRC01 cell ages are defined as young, with a seven to 10 population doubling level (PDL) and as standard with a 50 to 90 PDL. The standard PDL working cell bank was derived from the young PDL working cell bank.

## 2.1.1 | Pre-cultures

Working cell bank cells (1 mL frozen in liquid nitrogen) were thawed into 250 mL baffled, vented shake flasks with 70 mL working volume containing ActiPro media (GE Healthcare) with 6 mM L-glutamine (Sigma-Aldrich) and maintained in a 5%  $\rm CO_2$  incubator at 37°C with orbital shaking at 135 rpm. Cells were passaged five times, in the exponential growth phase (every 2–3 days) to a target cell density of 0.4 ×  $\rm 10^6$  cells mL<sup>-1</sup>, prior to inoculation into the ambr250 system.

#### 2.1.2 | Bioreactors

The ambr250 bioreactors (Sartorius Stedim, Göttingen, Germany) were equipped with two pitched blade impellers and an open pipe sparger (vessel part number: 001--5G25). The bioreactors were inoculated at a target cell density of  $0.4 \times 10^6$  cells mL $^{-1}$  in 210 mL total volume ActiPro media. The feeding began on Day 2.5 at 3% (v/v) for Cell Boost 7a and 0.3% (v/v) for Cell Boost 7b (GE Healthcare) with daily feeding, then increased according to the following percentages: Boost 7a (v/v)/Boost 7b (v/v); Day 5.5 to Day 6.5 – 4%/0.4%; Day 7.5 to Day 8.5 – 5%/0.5%. Glucose was supplemented daily, as needed, starting on Day 2.5, to maintain cultures above 4 g L $^{-1}$ . Cultures were stressed with 0 mM or 10 mM ammonium chloride in duplicate 12 h post-inoculation, where media was used to normalize the volume of the 0 mM (control) cultures to 10 mM ammonia-stressed cultures. Bioreactors were harvested on Day 8.5.

For the ambr250 bioreactors, the temperature was controlled to  $36.5^{\circ}$ C. The pH was controlled via sparging carbon dioxide and air, and a base addition via liquid pumps (1 M sodium bicarbonate). The pH setpoint was 7.0 with an initial deadband (DB) of 0.05 units, where the DB was changed to 0.01 at time 6.75 days. The base pump flow rate could vary from 0 to 10 mL min<sup>-1</sup> and the carbon dioxide gas flow rate could vary from 0 to 20 mL min<sup>-1</sup>. All gases were supplied through the open pipe sparger; initial flow rate of the sparged air was 2 mL min<sup>-1</sup>. A gas

overlay was not used. The dissolved oxygen (DO) was controlled to 50% of air saturation using a proportional-integral-derivative (PID) control algorithm using two levels. For the ambr250 the PID controller, Output was determined by the "Deviation" or difference from the setpoint (also called the error or deviation) by the following equation:

$$Output = k_P \left( Deviation + t_D \frac{d \left( Deviation \right)}{dt} + \frac{1}{t_I} \int Deviation \, dt \right)$$

The  $k_P$  is the proportional parameter;  $t_D$  is the derivative parameter;  $t_I$  is the integral parameter. The first level increased the flow rate of pure oxygen from 0 to 80 mL min<sup>-1</sup> ( $k_p$  0.03,  $t_D$  0 s,  $t_I$  500 s) where the air flow was maintained at 2 mL min<sup>-1</sup> and was changed to  $k_p$  0.04 and  $t_I$  150 s on Day 6.75. The second level increased the stir speed from 300 to 600 rpm ( $k_p$  3.5,  $t_D$  0 s,  $t_I$  250 s) and was changed to  $t_I$  200 s on Day 5.75, 300 to 900 rpm and  $t_I$  150 s on Day 6.75, and 300 to 800 rpm on Day 7.75.

## 2.2 | Analytical methods

## 2.2.1 | Off-line measurements

Samples were taken daily, pre-feeding, for VCD, cell viability, and glucose. Additionally, post-feed samples were taken for glucose, lactate, glutamine, glutamate, IgG, and ammonia. VCD and viability were measured using the trypan blue exclusion method using the Vi-Cell XR cell viability analyzer (Beckman Coulter, Brea, CA). Extracellular glucose, lactate, glutamine, glutamate, IgG, and ammonia concentrations were measured using a Cedex Bioanalyzer (Roche Diagnostics, Mannheim, Germany).

## 2.2.2 | Amino acid analysis

Samples were taken on nominal Days 0.5, 2.5, 5.5, and 8.5 (terms used for the remainder of the manuscript) for amino acid analysis corresponding to culture times 0.61, 2.64, 5.58, and 8.57 days, respectively. The samples were centrifuged at  $10,000\times g$  for 15 min at 4°C; the supernatant was aliquoted into three 200  $\mu$ L aliquots and frozen at -20°C. A capillary electrophoresis with high pressure mass spectrometry (CE-HPMS) analyzer (Rebel, 908 Devices, Boston, MA) was used to analyze the bioreactor supernatants from Days 0.5, 2.5, 5.5, and 8.5. A calibration curve was used that contained five standards at 5  $\mu$ M,  $10~\mu$ M,  $25~\mu$ M,  $50~\mu$ M, and  $100~\mu$ M. Bioreactor samples were analyzed in technical triplicates. All data processing from the CE-HPMS system was performed using 908 Devices, Inc., in-house software. [44,445]

Alanine for the young and standard PDL cultures was also measured by a gas chromatography-flame ionization detector (GC-FID) method. For the GC-FID method, supernatant was derivatized by using the EZ:faast amino acid analysis kit (Phenomenex, Torrance, CA). Standard solutions were prepared for alanine to a final concentration of 10 mM in water and pH adjusted to below pH 7.0. Samples were prepared by combining 150  $\mu$ L supernatant and 50  $\mu$ L of an internal standard (200

 $\mu\rm M$  norvaline). Sample derivatization was performed as per manufacturer instructions,  $^{[46]}$  and a standard curve was generated. Derivatized samples were injected into the GC-FID instrument (Agilent Technologies, 7890A GC system) equipped with an autosampler (Agilent Technologies, 7683B Series Injector) and a Zebron ZB-AAA 10 m x 0.25 mm capillary GC column using helium as the carrier gas (1.5 mL min $^{-1}$  constant flow). The initial column temperature was 60°C and increased by 32°C min $^{-1}$  to a final temperature of 320°C. The FID temperature was held at 320°C and 2  $\mu\rm L$  of sample was injected at 250°C with a split ratio of 1:15 using a 10  $\mu\rm L$  syringe.

## 2.2.3 | Glycosylation analysis

Samples for glycosylation analysis were harvested on Days 2.5, 5.5, and 8.5. Samples were collected and centrifuged at  $10,000 \times g$  for 15 min at 4°C; the supernatant was extracted and transferred to fresh tubes then frozen at -20°C. Cell debris were further removed from thawed supernatant containing IgG (up to 1 mL) by centrifugation at 3,200 x g for 10 min at 4°C. Protein A Agarose resin (1 mL, Pierce, ThermoFisher Scientific, Waltham, MA) in a 15 mL column (pre-equilibrated with 10 mL sterilized phosphate-buffered saline (PBS)) was used to capture up to 1 mg IgG from supernatant. Samples were washed thrice with 10 mL PBS to elute non-specifically bound proteins. The IgG was eluted using 10 mL elution buffer (100 mM glycine, pH = 2.75, filter sterilized), collected in 1 mL fractions. Protein-containing fractions were combined and concentrated to 100 µL via Amicon ultra-centrifugal filters (Millipore Sigma, Burlington, MA) with subsequent buffer exchange into 1.5 mL PBS, then re-concentrated to a final volume of 20-100 μL. Protein concentrations were determined via spectrophotometry at 280 nm (Denovix DS-11). The purified IgG was stored at -20°C until analyzed. Protein purity was confirmed via electrophoresis where the purified IgG (15  $\mu$ g) was run on a 12% Tris-Glycine gel in SDS buffer (225 V for 45 min). The gels were stained with Coomassie Brilliant blue (MP Biomedicals, Solon, OH) and de-stained with 30% methanol, 10% acetic acid. Gelanalyzer 2010a (gelanalyzer.com) was used to determine protein purity (all samples > 98%).

Glycan profiles were determined via ultra-performance liquid chromatography (UPLC). Glycans were released from the purified IgG and fluorescently labeled using the Glycoworks Rapifluor-MS N-glycan kit (Waters Corporation, Milford, MA) according to manufacturer's protocol. Labeled glycans were eluted from a BEH Amide column (1.7  $\mu$ m, 2.1 imes 150 mm) on a Waters ACQUITY ultra-performance liquid chromatography instrument using Waters universal N-glycan profiling method. The mobile phases were 50 mM ammonium formate (pH = 4) and 100% acetonitrile with a gradient from 25:75 formate: acetonitrile to 46:54 over 36.5 min for glycan elution and followed by 100:0 for 6.6 min to clean column, lastly the column was re-equilibrated at 25:75 for 11.9 min, as per the manufacturers method. Glycan identities were determined by using dextran standards (Rapifluor-MS Dextran calibration ladder, Waters Corporation, Milford, MA) to create a standard curve and comparing retention times of glycans against reference values in the "Glycostore" database (https://glycostore.org/). Empower  $3\,\mathrm{software}$  (Waters Corporation, Milford, MA) was used for all analysis of chromatograms, and glycosylation data were analyzed as normalized peak area.

## 2.2.4 RNA isolation and RNA-Seq analysis

Samples for transcriptome analysis by RNA sequencing (RNA-Seq) were taken from the duplicate standard-aged cultures at Days 0, 2.5, 5.5, and 8.5. for both the control and ammonia-stressed cultures. The samples were harvested as described above and the pellet was stored in  $500\,\mu\text{L}$  RNAprotect cell reagent (Qiagen, Valencia, CA) at -20° C until RNA extraction. Total RNA extraction was performed with the RNeasy Plus Mini kit (Qiagen) according to the manufacturer's recommended protocol. Quality and integrity were validated via spectrophotometry (NanoDrop 8000 UV-Vis, Thermo Scientific, MA) and automated electrophoresis (RNA 6000 Nano kit with the Agilent 2100 Bioanalyzer System, Agilent, Santa Clara, CA) respectively. All samples had RNA integrity numbers (RIN) values of greater than 9.7.

cDNA library construction was performed by Novogene (Davis, CA) using 1  $\mu$ g of RNA and an NEBNext Ultra II RNA Library Prep Kit for Illumina (cat# E7490, New England Biolabs, Ipswich, MA, USA) according to the manufacturer's protocol. The resulting 250–350 bp insert libraries were quantified using a Qubit 2.0 fluorometer (Thermo Fisher Scientific, Waltham, MA, USA) and quantitative PCR. Size distribution was analyzed using an Agilent 2100 Bioanalyzer (Agilent Technologies, Santa Clara, CA, USA). Qualified libraries were sequenced on an Illumina Novaseq 6000 Platform (Illumina, San Diego, CA, USA) using a paired-end 150 run (2  $\times$  150 bases). A minimum of 20 M raw reads were generated from each library.

Raw sequence reads were de-multiplexed on the instrument and reads  $\geq$  36 bp were cleaned of adapter and low-quality bases (< Phred 15) with the Trimmomatic (v0.38) software package. [47] Trimmed reads were aligned with the STAR (v2.7.1) software package [48] to the Chinese hamster reference genome (NCBI GCF\_003668045.1\_CriGri-PICR) and the sequence for the human VRC01 recombinant protein sequence (See the Supplemental Materials for the VRC01 heavy and light chain nucleotide sequences). The locally aligned sequences were then passed through samtools (v1.4)[49] to be viewed, sorted, indexed, and converted to BAM files for gene quantification using HTSeq (v0.11.2)[50] with default settings.

Raw data sets have been deposited into the Sequence Read Archive (SRA), part of the National Center for Biotechnology Information (NCBI) database, National Library of Medicine, National Institutes of Health. Sequence Read Archive (SRA) accession numbers for the 10 mM ammonia treated and 0 mM ammonia control group samples are SAMN13762555 – SAMN13762568 under BioProject number PRJNA599947.

## 2.3 | Differential expression gene analysis

The R/Bioconductor package, DESeq2 (v1.26.0),<sup>[51]</sup> was used for differential gene expression analysis. Briefly, DESeq2 performs an inter-

nal normalization to correct for library size and composition bias and fits the data to a generalized linear model (GLM) under a negative binomial distribution while controlling for dispersion and the inherent noisiness of genes with low read counts which complicate downstream analysis. For significance testing, DESeq2 can utilize either a likelihood ratio test (LRT) which compares a full and reduced model to test if removing predictor variables results in a statistically significant lesser fit or a Wald test which allows testing of individual coefficients. To address the multiple testing problem and reduce associated loss of power with the employed Benjamini-Hochberg procedure, the software conducts independent filtering to remove low count genes that have negligible chance of being detected as differentially expressed.

Through the DESeq2 pipeline, an initial inputted raw counts matrix of all genes in the appended reference genome was first passed through an LRT with model matrices:  $full = \sim ammonia \times day$ , and  $reduced = \sim day$ . Low count genes were automatically removed by independent filtering by a user-defined false discovery rate (FDR) of 0.05. Genes below the FDR cutoff were also required to be significant in at least one pairwise Wald comparison between the treated 10 mM NH $_3$  group and control 0 mM NH $_3$  group for Days 2.5, 5.5, and 8.5 (FDR < 0.05 and fold change (FC)  $\geq$  1.1).

## 2.4 | Specific consumption rates and specific productivity calculations

Specific consumption and production rates were estimated through an adapted linear model outlined in Meadows et al. (2008).<sup>[52]</sup> Measured metabolite concentrations were treated as the dependent variable, adjusted for feeding. Integral viable cell density (IVCD), calculated according to Pan et al. (2017),<sup>[53]</sup> was treated as the independent variable. Least squares regressions fits were used for each metabolite with time to calculate the specific consumption rates.

### 2.5 | Statistical analyses

Statistical analysis was performed using the software JMP Pro 14 (SAS Institute Inc., Cary, NC) on replicate data. Maximum cell concentration, cell viability, final IgG titer, and glycan data were analyzed using the Generalized Linear Model (p value  $\leq$  0.05) to determine if culture age/PDL, the ammonia concentration, or an interaction of the two were effectors. For effectors that were statistically significant, a Standard Least Square procedure (p value  $\leq$  0.05) with Tukey post-hoc analysis was conducted. The interaction term was removed from analysis if not significant. Specific consumption rates, specific productivity, and growth rate were calculated as linear regression slopes and analyzed through the same statistical procedure. The regression coefficients were used as the response variable, and the reciprocal of the variances were used as the weight to retain information about the strength of the relationship. Time intervals for linear regressions were: exponential growth phase (Days 0 - 4.5) and specific productivity (Days 0.5 -8.5). The specific consumption rates used time intervals with highest coefficient of determination for each metabolite. Standard-aged culture amino acid fluxes measured by CE-HPMS had time intervals from Days 0.5 – 5.5. The criteria for a non-zero slopes was then applied where fluxes were in the same direction (p value  $\leq$  0.1) and less than 0.1 pmol cell<sup>-1</sup> day<sup>-1</sup>. The Cauchy method was used to calculate the standard deviation for ratios, [54] such as the ratio of the titers between the control and ammonia-stressed cultures. Error bars on graphs represent standard deviations, unless stated otherwise. All averages are reported as mean  $\pm$  SD, unless stated otherwise.

#### 3 | RESULTS AND DISCUSSION

In previous studies, the effect of ammonia stress has been described for CHO cells with uncharacterized or unstated culture ages.  $^{[7,12,33]}$  It is now widely accepted that culture age or passage numbers/doublings, now more properly defined as the PDL,  $^{[55]}$  affects the capability of CHO cells to respond to stress.  $^{[56]}$  Recent work described the negative effects of ammonia on growth, product quantity, and productivity for cells with a standard PDL  $>50.^{[44]}$  In the present work, both young-aged cells, defined to be within 10 PDL of the original clone, and standard-aged cells (between 50 and 90 PDL) were cultured in parallel to determine the role cell age played in the response CHO cells had to an ammonia stress. The growth characteristics of these cultures are shown in Figure 1. Transcriptome analysis was also used to determine the underlying causes of metabolic shifts in amino acid metabolism observed in this study and elsewhere.  $^{[44]}$ 

# 3.1 | Cell growth and productivity under ammonia stress

Both young- and standard-aged CHO cell cultures were grown in parallel and stressed with a bolus of ammonium chloride at  $12\ h$  (Day 0.5), which increased the ammonia concentration by  $10\ mM$ . In all cultures the ammonia then increased from Days 0.5-1.5, due to the near equimolar glutamine consumption (Figure 1C). Ammonia consumption was observed in the ammonia-stressed cultures until Day 8.5. The rapid decrease in ammonia concentration suggests an ammonia-inducible metabolic detoxification mechanism to counter the stressor.

The exponential growth rates for the ammonia-stressed cultures were significantly lower than the control cultures (p value  $\leq$  0.05) (Figure 1A). However, the growth rates for the control cultures regardless of culture age were similar at  $0.033 \pm 0.001 \, h^{-1}$ . Additionally, the maximum viable cell densities (VCD) were significantly different by culture age and the ammonia stress (p value  $\leq$  0.05) with VCDs, while cell viabilities were not significantly different by either factor (p value > 0.05). These small differences in the growth rates resulted in the IVCD being significantly affected by culture age and the ammonia stress. Specifically, the IVCD was  $40\% \pm 8\%$  higher for the control cultures (p value  $\leq$  0.05) compared to the ammonia-stressed cultures (Figure S3), and  $9\% \pm 6\%$  higher for the young cultures (p value  $\leq$  0.05) compared to the standard-aged cultures.

Glucose was fed as needed to maintain the glucose concentration between 4 and 6 g L<sup>-1</sup>, starting Day 2.5 (Figure 1D). The ActiPro Boost 7a feed contains glucose, such that supplement glucose was only needed to raise the glucose concentration after Day 6. Only the batch medium contains glutamine, as indicated by the decreasing concentration from Day 0 to Day 4. Since Cell Boost 7b contains glutamate, the glutamate accumulation caused the glutamine accumulation later in the cultures (Figure 1G and 1H). For the ammonia-stressed cultures, glutamate accumulated more rapidly due to feeding since the feeding volume was preset and based on bioreactor volume and not VCD.

The final IgG titer was significantly lower for the ammonia-stressed cultures (p value  $\leq$  0.05); however, PDL was not a significant effector (p value > 0.05) (Figure 1F). The final IgG titers for the control cultures were  $1.48 \pm 0.20$  fold higher than the ammonia-stressed cultures. The cell specific productivity was not significantly different due to PDL or the ammonia stress (p value  $\leq$  0.05). Overall, these results highlight that the cultures were well-controlled and synchronized, such that the effect of ammonia on the cultures at the metabolic and transcriptome levels could be evaluated.

## 3.2 | Amino acid metabolic changes

Net specific consumption rates were calculated for all the cultures between Days 0.5 – 5.5, reflective of the time interval with divergent ammonia profiles. The combined effect of the volume-based feeding strategy and lower VCDs on metabolite concentration profiles was normalized to VCD to identify ammonia-induced metabolic shifts. Amino acid uptake and intracellular conversion are shown in Figure 2A along with glycolysis and the TCA cycle. Most of the 17 amino acids quantified did not have significantly different consumption rates due to the ammonia stress (p value > 0.05).

Normally alanine is consumed for biomass generation, as seen in the control cultures (Figure 1I); however, alanine was the only amino acid with a significantly higher net production rate in the ammonia-stressed cultures. The observed increase of  $8.93 \pm 0.18$  mM between Days 2.5 -5.5 was in excess of the amount fed during that time (only a 1.86 mM increase) (Figure 1I). Alanine concentrations were determined solely by GC-FID for the young PDL cultures, but by both GC-FID and CE-HPMS for the standard PDL cultures. To determine if the young PDL culture had similar behavior, both analysis methods need to be shown for the standard PDL cultures. Even though both methods use standard curves, the absolute values for the same sample are different by the two methods, yet qualitatively the young and standard PDL cultures had similar behavior with respect to alanine metabolism. Further, these observed alanine profiles agree with previous work using this cell line in the ambr250 under ammonia stress with a different feeding protocol (Figure S1) and consistent with other biological systems. [3,16,44,57-60]

Extracellular ammonia increased to 9.57  $\pm$  0.94 mM from the ammonium chloride bolus on Day 0.5 and further increased the following day presumably due to glutamine deamidation (Figure 1C). Ammonia concentrations then decreased until Day 5.5 in the stressed cultures with an observed change of -6.83  $\pm$  0.38 mM. In this same time

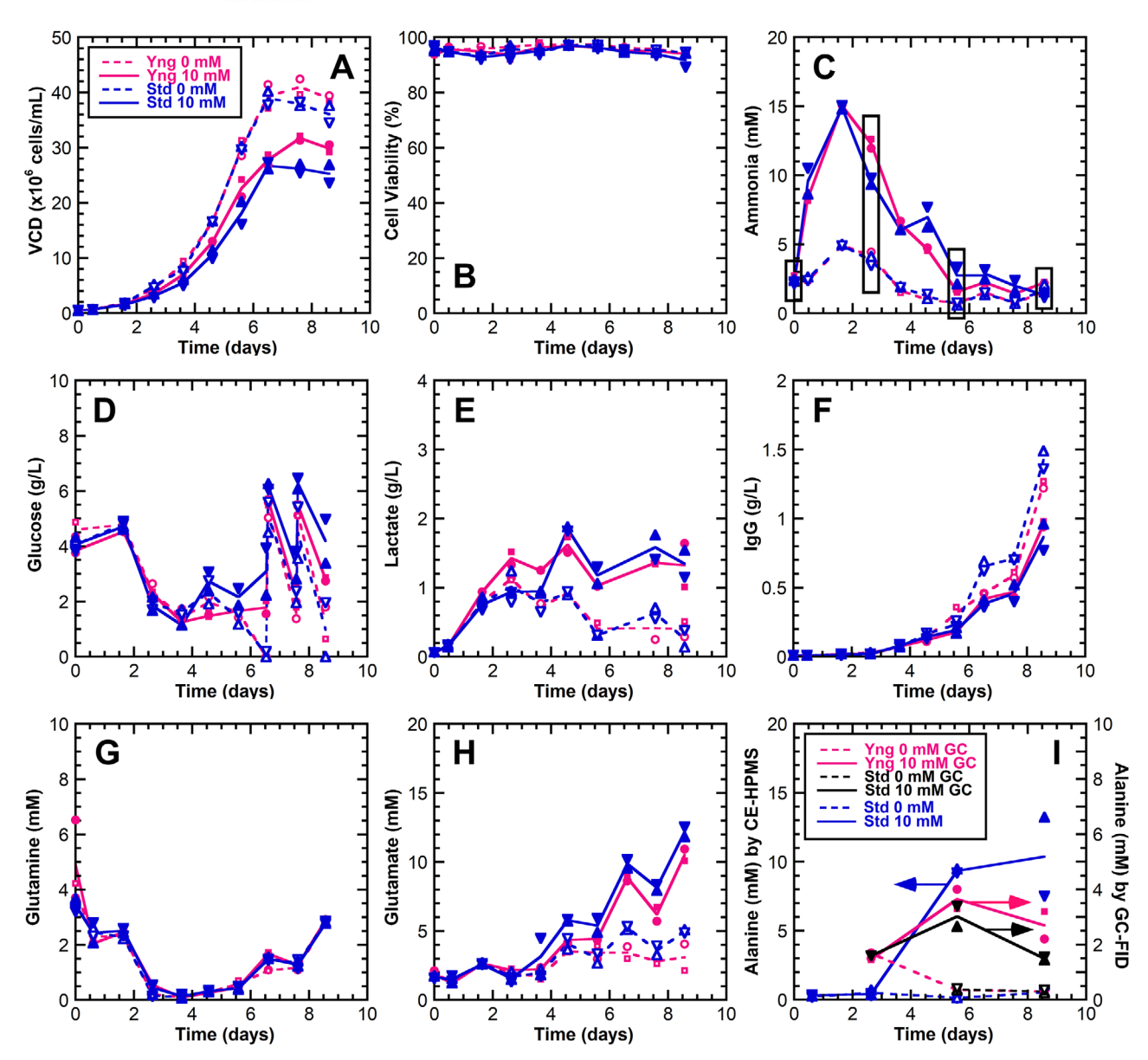


FIGURE 1 Growth and cell metabolite profiles. Control (0 mM) and 10 mM ammonia-stressed cultures of CHO VRC01 cells of young and standard PDL were examined, where the ammonia stress was added at 12 h. A. viable cell density (VCD); B. Cell viability; C. Ammonia; D. Glucose; E. Lactate; F. IgG (titer); G. Glutamine; H. Glutamate; and I. Alanine. Young PDL cultures are shown in magenta and the standard PDL cultures are shown in blue (except in the alanine panel (I), where black was used represent the standard PDL cultures measured by GC-FID). Dashed lines with hollow symbols represent the control cultures and solid lines with closed symbols represent the ammonia-stressed cultures. The sample times collected for the glycan and transcriptome analysis are shown in panel C. Only the standard culture was sampled for the transcriptome analysis. The lines represent the mean of duplicate cultures; all data points are shown

interval, alanine production adjusted for feed was nearly equimolar to ammonia consumption (7.06  $\pm$  0.18 mM); a relationship similarly observed by others. [3] Further, the specific production and consumption rates between Days 0.5 – 5.5 for alanine and ammonia are balanced (Figure 3).

Several other amino acids also had increased consumption rates due to the ammonia stress. Specifically, isoleucine, leucine, phenylalanine, serine, tryptophan, tyrosine, and valine all had increased consumption rates due to the ammonia stress (p value  $\leq$  0.1) (Figure 3) in agreement with the literature. [16,61] These seven amino acids have anaplerotic

roles that allow the TCA cycle to function as both a biosynthetic and a bioenergetic pathway.<sup>[61]</sup> Higher consumption rates would indicate ammonia disrupted the efficiency of central carbon metabolism and accelerated TCA turnover to meet energy demands. This was likely coupled with a disproportionate increase in energy expenditure and cataplerosis for cell maintenance requirements.

Previous research suggests the primary inhibitory mechanism from elevated ammonia is intracellular pH (pH $_{i}$ ) changes owing to the ionized and nonionized forms reestablishing equilibrium, following the outflow of the membrane-diffusible NH $_{3}$  (Figure 2A). [22,25,62,63]

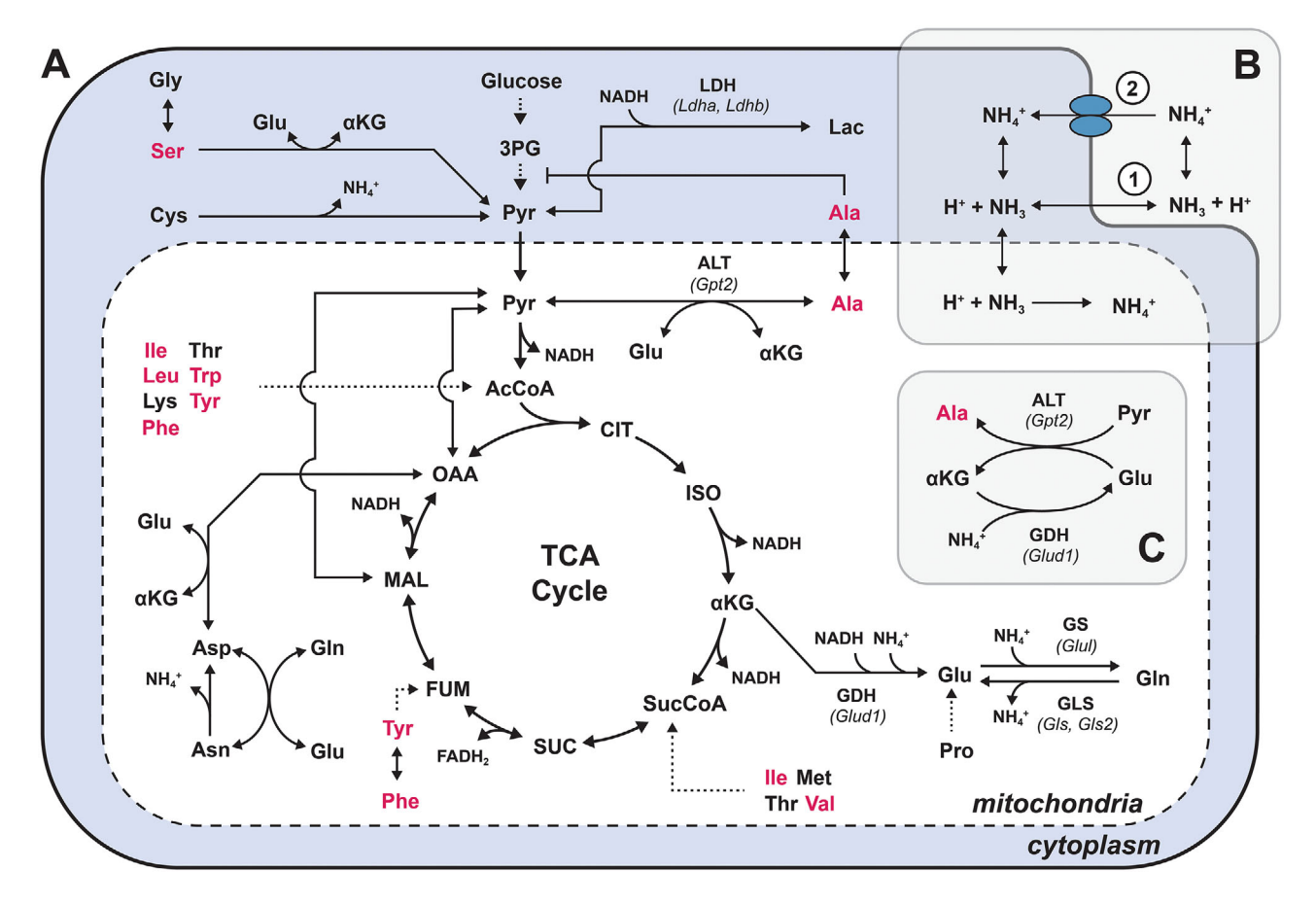


**FIGURE 2** Simplified metabolic pathways in CHO cells. (A) Major pathways. Amino acids with significant differences in specific consumption/production rates due to elevated ammonia are shown in red (p value  $\leq$  0.1). The common three letter abbreviations are used for all amino acids. (B) pH change mechanism by ammonia for cytoplasm and mitochondria. (1) Diffusion of NH<sub>3</sub> through membrane; (2) Active and facilitated transport of NH<sub>4</sub><sup>+</sup> by K<sup>+</sup> transporters. (C) Hypothesized ammonia detoxification method. Dotted lines represent multiple enzymes. Key ammonia detoxification enzymes are labelled with protein-coding gene italicized beneath

An ammonium chloride addition acidifies the cytoplasm and slightly alkalinizes the mitochondria. [22] Intracellular pH changes have been shown to affect several vital cell functions and bioprocess outcomes. [6,11,13,14,63] Without the capacity to utilize the urea cycle due to a lack of carbamoyl phosphate synthase gene expression, CHO cells must detoxify ammonia through alternative amino acid metabolism. [37–41]

Under ammonia stress, the CHO cells likely utilized a two-step detoxification pathway through the mitochondrial isozymes of glutamate dehydrogenase (GDH) and alanine transaminase (ALT), which generates alanine while consuming ammonium (Figure 2C). Specifically, GDH catalyzed  $\alpha$ -ketoglutarate ( $\alpha$ KG) + NH4+ + NADH to yield L-glutamate + NAD+. Further, alanine transaminase then catalyzed glutamate + pyruvate to generate alanine +  $\alpha$ -ketoglutarate ( $\alpha$ KG). GDH is a key metabolic regulator which facilitates carbon flow into the TCA cycle during restricted nutrient access. [61] The enzyme is highly sensitive to pH and ammonia concentrations, cited to reverse flux into a glutamate-producing reaction with elevated ammonia levels. [61,64] Additionally, the Michaelis-Menten constant (Km) for ammonia has been shown to increase several-fold from pH 8.0 to 7.0 in human GDH. [65] Under glucose-replete conditions, the synthesized gluta-

mate oxidizes primarily through transaminase reactions [26,66-68] The selected transamination pathway varies by biological system; however, CHO cells have been shown to predominately utilize ALT. [3,64,69] Taken together, the overall process shunted ammonium to alanine via pyruvate from the mitochondrial pool. [59,61] Consequently, there was a negligible change in net specific glutamate consumption under ammonia stress as restoration of  $\alpha$ KG is balanced by the equimolar ammonia consumption and alanine production. This mechanism of ammonia sequestration has been described in CHO cells and hybridoma lines. [3,64,69] Therefore, metabolic sequestration of ammonia primarily results in the formation of alanine, which serves as a nitrogen sink, but at the expense of mitochondrial pyruvate and NADH. [59,70] Consumption of these necessary reductants is a likely contributor to the overall inhibitory effects.

## 3.3 | Glycosylation changes due to ammonia stress

To evaluate the impact of ammonia stress on the glycosylation profiles of the VRCO1 antibody (IgG), both young and standard cells were evaluated at two time points (Days 5.5 and 8.5) (Figure 4A). The greatest

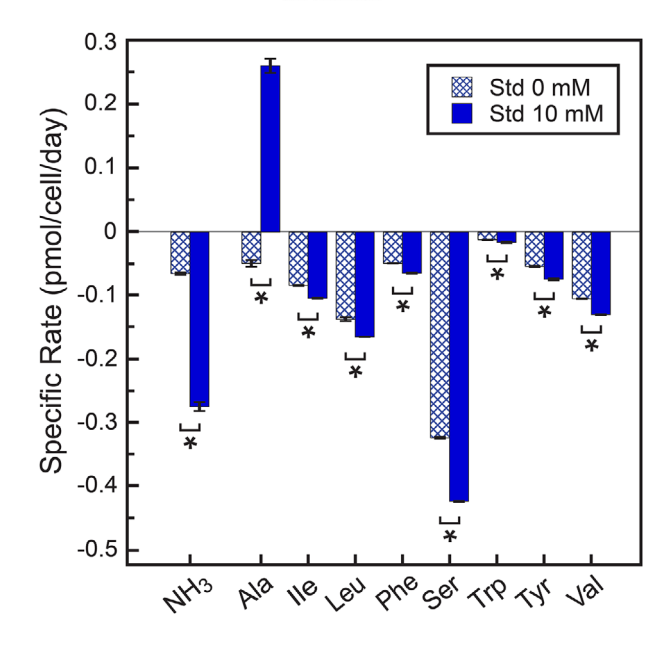


**FIGURE 3** Specific consumption and production rates for metabolites and amino acids between Days 0.5 – 5.5. consumption is shown as negative values and production is shown as positive values. Asterisks denote the difference was significance by both weighted least squares and slope test (p value  $\leq 0.1$ ). Error bars represent standard deviations

impact of ammonia stress on the glycosylation profile of the VRCO1 antibody was observed on Day 5.5, consistent with measured transient ammonia stress in the cultures prior to Day 5.5 (Figure 1). The glycosylation profile of VRCO1 from ammonia stress cultures on Day 8.5 was more similar to the unstressed cultures (Figure 4B), which is consistent with the lower observed ammonia concentrations at Day 8.5 (Figure 1).

The most apparent impact of the ammonia stress on Day 5.5 is the reduction in galactosylation observed for both young and standard PDL cultures (Figure 4B), consistent with previously published results.[71-74] The total galactosylation comprising species G1, G1F, G2, G2F, G1FS1, and G2FS1, and was reduced by the ammonia stress on Day 5.5 from 70% to 53% for the standard PDL cultures and 71% to 60% for the young PDL cultures (Figure 4B) (p value  $\leq$  0.05). The most highly changed species were G1F, G2F, and G2FS1 glycan species (p value  $\leq$  0.05) (Figure 4A). The terminal galactosylation comprising species G1, G1F, G2, and G2F was similarly reduced by the ammonia stress on Day 5.5 from 32% to 21% for the standard PDL cultures and 33% to 27% for the young PDL cultures (p value  $\leq$  0.05) (Figure 4B). The most highly changed species were G1F and G2F glycan species (p value ≤ 0.05) (Figure 4A). Galactosylation was also sensitive to culture age (p value  $\leq$  0.05), yet there was no significant interaction between culture age and the ammonia stress (p value > 0.05). A similar reduction in galactosylation is observed for persistent ammonia-stressed CHO VRC01 cultures with standard PDL, despite a different feeding and gassing protocol (Figure S2).<sup>[44]</sup> In this prior work, a higher ammonia stress of 30 mM further increased the trend of reduced galactosylation (Figure S2).[44]

Ammonia stress slightly reduced sialylation on Day 5.5 for standard-(from 38% to 32%) and young-aged (from 37% to 34%) cultures (p value  $\leq$  0.05) (Figure 4B). The most highly changed species was G2FS1 (p value  $\leq$  0.05) (Figure 4A), which also is consistent with previous work. [11.12.14.31.33.75.76] Overall, culture age affected sialylation under ammonia stress (p value  $\leq$  0.05), but this was less pronounced compared to the galactosylation changes. By Day 8.5, there was no significant difference in sialylation for either young- or standard-aged cultures (p value > 0.05) (Figure 4A). Yet, the G2S1 glycan species, overall, had lower levels on Day 8.5 compared to Day 5.5 (p value  $\leq$  0.05). Similarly, G2FS1 was observed to be reduced in the persistent ammonia stress culture, but not for the G2S1 glycan species at the same time (Figure S2). The higher ammonia stress (30 mM) further increased the sialylation reduction (Figure S2). [44]

Fucosylation was significantly impacted by both cell age and ammonia stress, where young PDL and ammonia-stressed cultures had lower levels of fucosylated glycans (p value  $\leq$  0.05) (Figure 4B). There was no observed interaction effect between cell age and ammonia. A significant reduction in fucosylated glycans was also observed in the persistent ammonia-stressed cultures, and was increased in the 30 mM ammonia-stressed standard-aged cultures (Figure S2). The presence of G1 glycan species was under 2% of all glycans for all treatments of young PDL cells. Interestingly, regardless of treatment, all standard PDL cultures lacked detectable G1 glycan species and had slightly elevated G0F compared to the young PDL cultures.

## 3.4 | Evaluation of gene expression changes

To elucidate the underlying mechanisms of alanine metabolism and glycosylation changes in ammonia-stressed CHO cell cultures, transcriptome analysis via RNA-Seg was performed on the standard-aged cultures. Significance testing on the original 32,430 genes present in the reference genome and VRC01 plasmid yielded 12,520 genes with mean normalized expression levels above the software's calculated filter threshold of 23.15. Principal component analysis (PCA) resulted in two significant dimensions to these 12,520 genes (Figure 5B). The greatest amount of variance (72%) was attributed to the growth phase, as both the control and ammonia-stressed cultures follow identical distributions clustering vertically along PC1 for any given day. The second dimension highlighted the effect of the ammonia stress, as all changes were in the same direction due to the ammonia stress, downward along the y-axis; however, this dimension accounted for a much lower variance (9%) than the growth phase. Between the control and ammoniastressed cultures on Days 5.5 and 8.5, there was a reduced variation on PC2 on Day 8.5 complementing the ammonia profiles of these cultures. The shape of the PCA suggested the ammonia stress had a transient effect on the transcriptome, which was partially reversed by Day 8.5 relative to Day 5.5. Further, even at Day 2.5, which was approximately 48 h after the ammonia stress, the transcriptome was fairly stable for the control cultures, but only slightly affected by the ammonia stress, relative to the Day 5.5 and 8.5 samples. A LRT was then used to identify 4584 significant genes where the FDR was below the

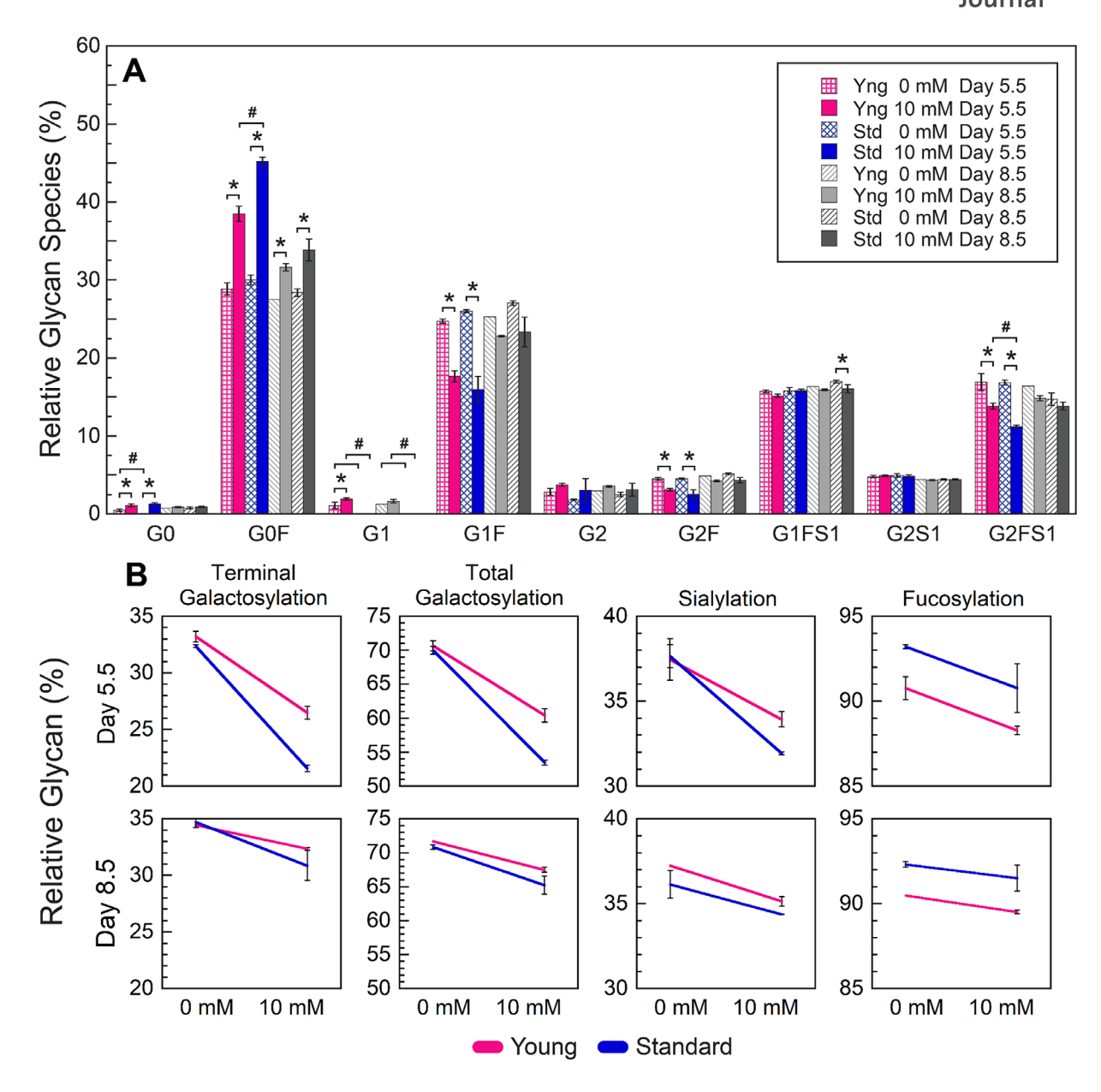


**FIGURE 4** Glycan profiles for the Control (0 mM ammonia) and 10 mM ammonia stress of young and standard-aged CHO VRC01 cultures. (A) Overall glycan profile. Shaded bars represent the control cultures and solid bars represent the ammonia-stressed cultures. Young PDL cultures are shown in magenta (Day 5.5) or lighter grey (Day 8.5) and the standard PDL cultures are shown in blue (Day 5.5) or darker gray (Day 8.5). Data is mean  $\pm$  SD of n=2 biological replicates (n=1 biological replicate for young PDL control). Asterisks denote statistical significance (p value  $\leq$  0.05) when comparing control to ammonia-stressed cultures. Hash mark denotes statistical significance (p value  $\leq$  0.05) when comparing young vs. standard PDL cultures. (B) Trends in glycosylation profile. Young PDL cultures shown in Magenta, standard PDL cultures shown in blue

cutoff of 0.05. This approach was used to reduce identifying genes which were mostly affected by cell cycle, as most of the variance was cell cycle related. In Figure S4, a summary of the cell cycle genes are profiled, which uniformly had differential expression across the cultures, yet the trends are ammonia stress independent. An additional Wald pairwise comparison criterion (FDR  $\leq$  0.05, fold change (FC)  $\geq$  1.1) yielded a significant gene list of 1362 genes, which represents a comparison of the control and ammonia-stressed cultures at the same time point. In the Supplemental Materials, a list of the 64 genes with FC  $\geq$  1.5 (FDR  $\leq$  0.05) is provided, as FC  $\geq$  1.1 is rather relaxed.

The 1362 gene list was used to analyze glycosylation and amino acid metabolism related genes, in order to provide the most comprehensive examination.

## 3.4.1 | Glycosylation-related genes

Of special interest within the transcriptome analysis were glycosylation-related genes. Of the 300 unique glycosylation-related genes identified by Xu (2011), 173 genes had expression under these

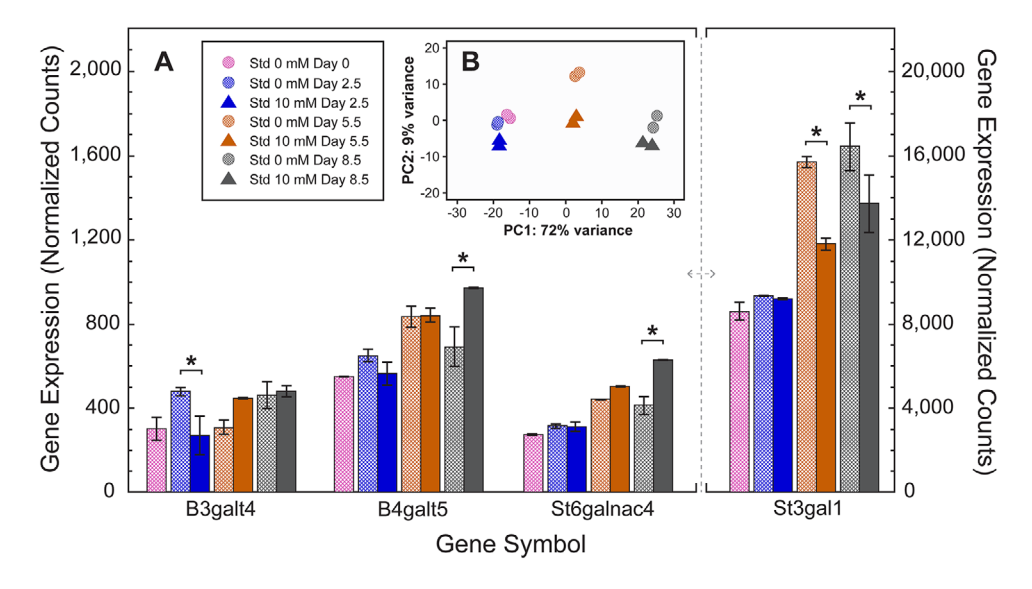


**FIGURE 5** Gene expression profiles for glycosylation-related genes for galactosylation and sialylation. (A) Normalized counts for two galactosyltransferase genes, B3galt4 and B4galt5, and the sialyltransferase gene, St6galnac4, shown on the left-axis. St3gal1 sialyltransferase gene expression shown on the right-axis. Asterisks denote significantly differentially expressed genes in the likelihood ratio test (LRT) (FDR  $\leq$  0.05) and with at least one Wald pairwise contrast between treatments (FDR  $\leq$  0.05). Error bars represent standard deviations. (B) Principal component analysis (PCA) plot of the 12,520 significant genes

bioreactor conditions. [77] Further, 39 additional genes were observed to have expression with names similar to those previously identified as glycosylation genes. The initial screening of these 212 genes with the LRT (FDR  $\leq$  0.05), identified 101 genes with differential expression. A Wald pairwise test criteria (FDR  $\leq$  0.05, FC  $\geq$  1.1) was used to compare the control and ammonia-stressed cultures at the same time point. This reduced the glycosylation-related genes sensitive to the ammonia stress to 25 significant genes out of the 339 genes.

While 25 glycosylation-related genes were observed to have differential expression, the primary genes associated with galactosylation were not significantly affected. Overall, the alterations observed in the galactosylation due to ammonia stress were most likely due to posttranslational activity differences. While the primary galactosyltransferase gene, B4galt1, and galactosidase genes were not differentially expressed, two analogs, B3galt4, B4galt5, were found to have significantly reduced expression on Day 2.5, but had increased expression on Day 8.5, respectively (Figure 5A). Conversely, two sialyltransferase genes (St3gal1, St6galnac4) had significant differential expression due to the ammonia stress; decreased expression on Day 5.5 and increased expression on Day 8.5, respectively. These sialylation related genes had behavior that corresponds with the observed protein sialylation levels (Figure 4B). The lower sialylation observed on Day 5.5 could be attributed to the significantly reduced St3gal1 expression due to the ammonia stress. Several other glycosylation-related genes including mannosidase, mannosyltransferase, GlcNAc-transferases, lysosomal enzymes, N-glycans-transferase, hexosaminidases, sulfatases, sulfotransferases, nucleotide sugar transporters, and nucleotide synthesis genes had differential expression. As fold change cannot accurately express the differential expression due to the overrepresentation of low count genes, a normalized counts bar chart has been included in the Supplemental Materials (Figure S5). The aggregate effect of

these differentially expressed genes could have played a role in the decreased glycosylation quality.

#### 3.4.2 | Alanine biosynthesis

Past work has examined potential metabolic mechanisms of alanine accumulation, but lacked transcriptome analysis. [7,44,59] While there are two potential alanine anabolism reactions in CHO cells, the L-alanine degradation via transaminase is the only reaction pathway that has been observed with measurable gene expression for CHO cells (Figure 2A).[78,79] The alternative alanine-glyoxylate transaminase enzyme has not been observed under several bioreactor conditions,<sup>[78,79]</sup> including this study. Under ammonia stress, only the mitochondrial isozyme of alanine transaminase encoded by the Gpt2 gene was observed to have measurable gene expression; however, this gene did not have significantly different gene expression between the control and ammonia-stressed cultures. The specific consumption and production rates for NH<sub>3</sub>, alanine, and glutamate were significantly different (Figure 2C and Figure 3). Yet, none of the seven genes responsible for NH<sub>3</sub>, alanine, and glutamate reactions had differential expression due to the ammonia stress (Figure 2). This would indicate that L-alanine degradation via the transaminase pathway is most likely substrate-level controlled, even under ammonia stress.

#### 4 | CONCLUDING REMARKS

This work reports the first study directly comparing the combined effect of cell line age and ammonia stress on CHO cells. The moderate ammonia stress, given as a bolus early in the cultivation, resulted in transitory elevated ammonia. The bioprocess and glycosylation analysis were consistent with previous studies. Under the control conditions, the older (standard PDL) cell line performs nearly identical to the younger cell line (young PDL). It was not until the cultures were ammonia-stressed that significant glycosylation differences were observed due to culture age, where the standard PDL culture was more negatively affected. Further, the cell age contributed to lower maximum VCD, yet not a difference in cell viability. Plus, the IgG production was lower overall, but rather similar on a cell specific level. To better understand the age related changes, metabolite analysis was used, and indicated that alanine production was a primary mechanism used by the cultures for ammonia detoxification by converting the intracellular ammonium and pyruvate pools into alanine. Interestingly, RNA-Seq transcriptomic analysis on the standard PDL cultures indicated that alanine production is not controlled at the mRNA leveTl, as no significant changes in alanine metabolism related genes were observed. Overall, the transcriptome was remarkably stable due to ammonia stress. Likewise, the observed differences in glycosylation could not be directly attributed to changes in primary glycosylation gene expression levels.

#### **ACKNOWLEDGMENTS**

This work was funded by the National Science Foundation OIA-1736123. The authors thank Mr. Thomas Caldwell in Clemson's Department Bioengineering for assistance with the GC-FID analysis. The authors thank Evan Wells for his help with glycan analysis. The authorsthank 908 Devices for providing the CE-HPMS amino acid analysis.

#### **CONFLICT OF INTEREST**

The authors declare no financial or commercial conflict of interest.

## **AUTHOR CONTRIBUTIONS**

Benjamin F. Synoground: Data curation; Formal analysis; Investigation; Methodology; Validation; Visualization; Writing-original draft; Writing-review & editing. Christina Leuze: Investigation; Methodology

## DATA AVAILABILITY STATEMENT

The data that support the findings of this study are openly available in the NCBI sequence read archive (SRA) under the accession numbers SAMN13762555 - SAMN13762568.

#### ORCID

Nicholas R. Sandoval https://orcid.org/0000-0002-1743-3975

## REFERENCES

- Kovacevic, Z., & McGivan, J. D. (1983). Mitochondrial metabolism of glutamine and glutamate and its physiological significance. *Physiological Reviews*, 63, 547–605.
- Pereira Sara, Kildegaard Helene Faustrup, Andersen Mikael Rørdam, Impact of CHO Metabolism on Cell Growth and Protein Production: An Overview of Toxic and Inhibiting Metabolites and Nutrients Biotechnology Journal 2018, 13, 1700499. http://doi.org/10.1002/biot. 201700499.

- Li, J., Wong, C. L., Vijayasankaran, N., Hudson, T., & Amanullah, A. (2012). Feeding lactate for CHO cell culture processes: impact on culture metabolism and performance. *Biotechnology and Bioengineering*, 109, 1173–1186.
- Butler, M., Hassell, T., Doyle, C., Gleave, S., Jennings, P. (1991). European society for animal cell technology, in: Spier, R. E., Griffiths, J. B., Meignier, B. (Eds.), General meeting (10th: 1990: Avignon, France), Butterworth-Heinemann Ltd, Oxford.
- Xu, S., Gavin, J., Jiang, R. B., Chen, H. (2017). Bioreactor productivity and media cost comparison for different intensified cell culture processes. *Biotechnology Progress*, 33, 867–878.
- Fan, Y., Del Val, I. J., Muller, C., Sen, J. W., Rasmussen, S. K., Kontoravdi, C., Weilguny, D., & Andersen, M. R. (2015). Amino acid and glucose metabolism in fed-batch CHO cell culture affects antibody production and glycosylation. *Biotechnology and Bioengineering*, 112, 521–535.
- McAtee Pereira A. G., Walther J. L., Hollenbach M., Young J. D., 13C flux analysis reveals that rebalancing medium amino acid composition can reduce ammonia production while preserving central carbon metabolism of CHO cell cultures *Biotechnology Journal* 2018, 13, 1700518. http://doi.org/10.1002/biot.201700518.
- Le, H., Kabbur, S., Pollastrini, L., Sun, Z. R., Mills, K., Johnson, K., Karypis, G., & Hu, W. S. (2012). Multivariate analysis of cell culture bioprocess data-Lactate consumption as process indicator. *Journal of Biotechnology*, 162, 210–223.
- Lao, M. S., & Toth, D. (1997). Effects of ammonium and lactate on growth and metabolism of a recombinant Chinese hamster ovary cell culture. *Biotechnology Progress*, 13, 688–691.
- Chitwood, D. G., Wang, Q., Elliott, K., Bullock, A., Jordana, D., Li, Z., Wu, C., Harcum, S. W., & Saski, C. A. (2021). Characterization of metabolic responses, genetic variations, and microsatellite instability in ammonia-stressed CHO cells grown in fed-batch cultures. BMC Biotechnology [Electronic Resource], 21, 4.
- Andersen, D. C., & Goochee, C. F. (1995). The effect of ammonia on the O-linked glycosylation of granulocyte-colony-stimulating factor produced by Chinese-hamster ovary cells. Biotechnology and Bioengineering, 47, 96–105.
- Chen, P. F., & Harcum, S. W. (2006). Effects of elevated ammonium on glycosylation gene expression in CHO cells. *Metabolic Engineering*, 8, 123–132.
- Butler, M., & Spier, R. E. (1984). The effects of glutamine utilisation and ammonia production on the growth of BHK cells in microcarrier cultures. *Journal of Biotechnology*, 1, 187–196.
- Yang, M., & Butler, M. (2000). Effects of ammonia on CHO cell growth, erythropoietin production, and glycosylation. *Biotechnology and Bio*engineering, 68, 370–380.
- Lee, J. H., Kim, J., Park, J.-H., Heo, W. D., & Lee, G. M. (2019). Analysis of Golgi pH in Chinese hamster ovary cells using ratiometric pH-sensitive fluorescent proteins. *Biotechnology and Bioengineering*, 116, 1006–1016.
- Ozturk, S. S., Riley, M. R., & Palsson, B. O. (1992). Effects of ammonia and lactate on hybridoma growth, metabolism, and antibody production. Biotechnology and Bioengineering, 39, 418–431.
- Post, R. L., & Jolly, P. C. (1957). The linkage of sodium, potassium, and ammonium active transport across the human erythrocyte membrane. *Biochimica etBiophysica Acta*, 25, 118–128.
- Good, D. W., Knepper, M. A., & Burg, M. B. (1984). Ammonia and bicarbonate transport by thick ascending limb of rat kidney. *American Jour*nal of Physiology, 247, F35–F44.
- Kikeri, D., Sun, A., Zeidel, M. L., & Hebert, S. C. (1989). Cell membranes impermeable to NH3. *Nature*, 339, 478–480.
- Müller, T., Walter, B., Wirtz, A., & Burkovski, A. (2006). Ammonium toxicity in bacteria. Current Microbiology, 52, 400–406.
- 21. Dai, X., Hu, C., Zhang, D., Dai, L., & Duan, N. (2017). Impact of a high ammonia-ammonium-pH system on methane-producing archaea

- and sulfate-reducing bacteria in mesophilic anaerobic digestion. *Bioresource Technology*, 245, 598–605.
- Martinelle, K., & Häggström, L. (1993). Mechanisms of ammonia and ammonium ion toxicity in animal cells: Transport across cell membranes. *Journal of Biotechnology*, 30, 339–350.
- 23. Busa, W. B. (1986). Chapter 16 The Proton as an Integrating Effector in Metabolic Activation, in: Kleinzeller, A., Bronner, F., Aronson, P. S., Boron, W. F. (Eds.), *Current Topics in Membranes and Transport*, Academic Press, pp. 291–305.
- Trivedi, B., & Danforth, W. H. (1966). Effect of pH on the kinetics of frog muscle phosphofructokinase. *Journal of Biological Chemistry*, 241, 4110–4112.
- Glacken, M. W., Adema, E., & Sinskey, A. J. (1988). Mathematical descriptions of hybridoma culture kinetics: I. Initial metabolic rates. *Biotechnology and Bioengineering*, 32, 491–506.
- Katunuma, N., Okada, M., & Nishii, Y. (1966). Regulation of the urea cycle and TCA cycle by ammonia. Advances in Enzyme Regulation, 4, 317–336.
- Berg, J. M., Tymoczko, J. L., & Stryer, L. (2002). Biochemistry, Fifth Edition, W.H. Freeman.
- 28. Freund, N. W., & Croughan, M. S. (2018). A simple method to reduce both lactic acid and ammonium production in industrial animal cell culture. *International Journal of Molecular Sciences*, 19.
- Ryll, T., Valley, U., & Wagner, R. (1994). Biochemistry of growth inhibition by ammonium ions in mammalian cells. *Biotechnology and Bioengineering*, 44, 184–193.
- 30. Genzel, Y., Ritter, J. B., Konig, S., Alt, R., & Reichl, U. (2005). Substitution of glutamine by pyruvate to reduce ammonia formation and growth inhibition of mammalian cells. *Biotechnology Progress*, 21, 58–69.
- 31. Yang, M., & Butler, M. (2002). Effects of ammonia and glucosamine on the heterogeneity of erythropoietin glycoforms. *Biotechnology Progress*, 18, 129–138.
- Ha, T. K., & Lee, G. M. (2015). Glutamine substitution: the role it can play to enhance therapeutic protein production. *Pharmaceutical Biopro*cessing. 3, 249–261.
- Ha, T. K., Kim, Y. G., & Lee, G. M. (2015). Understanding of altered Nglycosylation-related gene expression in recombinant Chinese hamster ovary cells subjected to elevated ammonium concentration by digital mRNA counting. *Biotechnology and Bioengineering*, 112, 1583– 1593.
- Ha, T. K., & Lee, G. M. (2014). Effect of glutamine substitution by TCA cycle intermediates on the production and sialylation of Fc-fusion protein in Chinese hamster ovary cell culture. *Journal of Biotechnology*, 180, 23–29.
- Kim, D. Y., Chaudhry, M. A., Kennard, M. L., Jardon, M. A., Braasch, K., Dionne, B., Butler, M., & Piret, J. M. (2013). Fed-batch CHO cell t-PA production and feed glutamine replacement to reduce ammonia production. *Biotechnology Progress*, 29, 165–175.
- Altamirano, C., Paredes, C., Cairo, J. J., & Godia, F. (2000). Improvement of CHO cell culture medium formulation: Simultaneous substitution of glucose and glutamine. *Biotechnology Progress*, 16, 69–75.
- Park, H. S., Kim, I. H., Kim, I. Y., Kim, K. H., & Kim, H. J. (2000). Expression
  of carbamoyl phosphate synthetase I and ornithine transcarbamoylase
  genes in Chinese hamster ovary dhfr-cells decreases accumulation of
  ammonium ion in culture media. *Journal of Biotechnology*, 81, 129–140.
- Ley, D., Pereira, S., Pedersen, L. E., Arnsdorf, J., Hefzi, H., Davy, A. M., Ha, T. K., Wulff, T., Kildegaard, H. F., & Andersen, M. R. (2019). Reprogramming AA catabolism in CHO cells with CRISPR/Cas9 genome editing improves cell growth and reduces byproduct secretion. *Metabolic Engineering*, 56, 120–129.
- Kim, N., Lee, Y., Kim, H., Choi, J., Kim, J., Chang, K. H., Kim, J. H., & Kim, H. J. (2004). Enhancement of erythropoietin production from Chinese hamster ovary (CHO) cells by introduction of the urea cycle enzymes, carbamoyl phosphate synthetase I and ornithine transcarbamylase. *Journal of Microbiology and Biotechnology*, 14, 844–851.

- Kim, H. J., & Kim, H.-J. (2006). Glycosylation variant analysis of recombinant human tissue plasminogen activator produced in urea-cycle-enzyme-expressing Chinese hamster ovary (CHO) cell line. *Journal of Bioscience and Bioengineering*, 102, 447–451.
- Chung, M. I., Lim, M. H., Lee, Y. J., Kim, I. H., Kim, I. Y., Kim, J. H., Chang, K. H., & Kim, H. J. (2003). Reduction of ammonia accumulation and improvement of cell viability by expression of urea cycle enzymes in Chinese hamster ovary cells. *Journal of Microbiology and Biotechnology*, 13, 217–224.
- Chen, P. F., & Harcum, S. W. (2007). Differential display identifies genes in Chinese hamster ovary cells sensitive to elevated ammonium. Applied Biochemistry and Biotechnology, 141, 349–359.
- Mulukutla, B. C., Mitchell, J., Geoffroy, P., Harrington, C., Krishnan, M., Kalomeris, T., Morris, C., Zhang, L., Pegman, P., & Hiller, G. W. (2019). Metabolic engineering of Chinese hamster ovary cells towards reduced biosynthesis and accumulation of novel growth inhibitors in fed-batch cultures. *Metabolic Engineering*, 54, 54–68.
- Elliott, K., Anderson, J., Gavin, C., Blakeman, K., Harcum, S., & Harris, G. (2020). Spent media analysis with an integrated CE-MS analyzer of Chinese hamster ovary cells grown in an ammonia-stressed parallel microbioreactor platform. *BioProcess Journal*, 19.
- Gilliland, W. M., & Ramsey, J. M. (2018). Development of a microchip CE-HPMS platform for cell growth monitoring. *Analytical Chemistry*, 90, 13000–13006.
- 46. Badawy, A.-B., Morgan, C., & Turner, J. (2008). Application of the Phenomenex EZ: faast™ amino acid analysis kit for rapid gaschromatographic determination of concentrations of plasma tryptophan and its brain uptake competitors. Amino Acids, 34, 587–596.
- 47. Bolger, A. M., Lohse, M., & Usadel, B. (2014). Trimmomatic: a flexible trimmer for Illumina sequence data. *Bioinformatics*, 30, 2114–2120.
- Dobin, A., Davis, C. A., Schlesinger, F., Drenkow, J., Zaleski, C., Jha, S., Batut, P., Chaisson, M., & Gingeras, T. R. (2013). STAR: ultrafast universal RNA-seq aligner. *Bioinformatics*, 29, 15–21.
- 49. Li, H., Handsaker, B., Wysoker, A., Fennell, T., Ruan, J., Homer, N., Marth, G., Abecasis, G., & Durbin, R. (2009). The sequence alignment/map format and SAMtools. *Bioinformatics*, 25, 2078–2079.
- Anders, S., Pyl, P. T., & Huber, W. (2015). HTSeq-a Python framework to work with high-throughput sequencing data. *Bioinformatics*, 31, 166–169.
- Love, M. I., Huber, W., & Anders, S. (2014). Moderated estimation of fold change and dispersion for RNA-seq data with DESeq2. *Genome Biology*, 15, 550.
- Meadows, A. L., Kong, B., Berdichevsky, M., Roy, S., Rosiva, R., Blanch, H. W., & Clark, D. S. (2008). Metabolic and morphological differences between rapidly proliferating cancerous and normal breast epithelial cells. *Biotechnology Progress*, 24, 334–341.
- Pan, X., Streefland, M., Dalm, C., Wijffels, R. H., & Martens, D. E. (2017).
   Selection of chemically defined media for CHO cell fed-batch culture processes. Cytotechnology, 69, 39–56.
- Hayya, J., Armstrong, D., & Gressis, N. (1975). Ratio of 2 normally distributed variables. *Management Science Series A-Theory*, 21, 1338– 1341
- Hayflick, L. (1973). Tissue Culture Methods and Applications, New York: Academic Press.
- Dahodwala, H., & Lee, K. H. (2019). The fickle CHO: a review of the causes, implications, and potential alleviation of the CHO cell line instability problem. *Current Opinion in Biotechnology*, 60, 128– 137.
- Sellick, C. A., Croxford, A. S., Maqsood, A. R., Stephens, G., Westerhoff, H. V., Goodacre, R., & Dickson, A. J. (2011). Metabolite profiling of recombinant CHO cells: Designing tailored feeding regimes that enhance recombinant antibody production. *Biotechnology and Bioengineering*, 108, 3025–3031.
- Sellick, C. A., Croxford, A. S., Maqsood, A. R., Stephens, G. M., Westerhoff, H. V., Goodacre, R., & Dickson, A. J. (2015). Metabolite profil-

- ing of CHO cells: Molecular reflections of bioprocessing effectiveness. *Biotechnology Journal*. 10. 1434–1445.
- Duarte, T. M., Carinhas, N., Barreiro, L. C., Carrondo, M. J. T., Alves, P. M., & Teixeira, A. P. (2014). Metabolic responses of CHO cells to limitation of key amino acids. *Biotechnology and Bioengineering*, 111, 2095–2106
- Hansen, H. A., & Emborg, C. (1994). Influence of ammonium on growth, metabolism, and productivity of a continuous suspension Chinese hamster ovary cell culture. *Biotechnology Progress*, 10, 121–124.
- Yang, C., Ko, B., Hensley, C. T., Jiang, L., Wasti, A. T., Kim, J., Sudderth, J., Calvaruso, M. A., Lumata, L., Mitsche, M., Rutter, J., Merritt, M. E., & DeBerardinis, R. J. (2014). Glutamine oxidation maintains the TCA cycle and cell survival during impaired mitochondrial pyruvate transport. *Molecular Cell*, 56, 414–424.
- 62. McQueen, A., & Bailey, J. E. (1990). Effect of ammonium ion and extracellular pH on hybridoma cell metabolism and antibody production. *Biotechnology and Bioengineering*, 35, 1067–1077.
- Wu, P., Ray, N. G., & Shuler, M. L. (1993). A computer model for intracellular pH regulation in Chinese hamster ovary cells. *Biotechnology Progress*, 9, 374–384.
- Ghorbaniaghdam, A., Chen, J., Henry, O., & Jolicoeur, M. (2014).
   Analyzing clonal variation of monoclonal antibody-producing CHO cell lines using an in silico metabolomic platform. *PLoS One*, 9, e90832.
- Zaganas, I., Pajęcka, K., Wendel Nielsen, C., Schousboe, A., Waagepetersen, H. S., & Plaitakis, A. (2013). The effect of pH and ADP on ammonia affinity for human glutamate dehydrogenases. *Metabolic Brain Disease*, 28, 127–131.
- Yang, C., Sudderth, J., Dang, T., Bachoo, R. M., McDonald, J. G., & DeBerardinis, R. J. (2009). Glioblastoma cells require glutamate dehydrogenase to survive impairments of glucose metabolism or Akt signaling. *Cancer Research*, 69, 7986–7993.
- Jenkins, H. A., Butler, M., & Dickson, A. J. (1992). Characterization of glutamine metabolism in two related murine hybridomas. *Journal of Biotechnology*, 23, 167–182.
- Street, J. C., Delort, A. M., Braddock, P. S., & Brindle, K. M. (1993). A 1H/15N n.m.r. study of nitrogen metabolism in cultured mammalian cells. *Biochemical Journal*, 291 (Pt 2), 485–492.
- Bonarius, H. P. J., Houtman, J. H. M., de Gooijer, C. D., Tramper, J., & Schmid, G. (1998). Activity of glutamate dehydrogenase is increased in ammonia-stressed hybridoma cells. *Biotechnology and Bioengineering*, 57, 447–453.
- Ben Yahia, B., Gourevitch, B., Malphettes, L., & Heinzle, E. (2017). Segmented linear modeling of CHO fed-batch culture and its application to large scale production. *Biotechnology and Bioengineering*, 114, 785–797.
- 71. Gawlitzek, M., Ryll, T., Lofgren, J., & Sliwkowski, M. B. (2000). Ammonium alters N-glycan Structures of Recombinant TNFR-IgG: Degrada-

- tive Versus Biosynthetic Mechanisms. Biotechnology & Bioengineering, 68, 637–646
- Hong, J. K., Cho, S. M., & Yoo, S. K. (2010). Substitution of glutamine by glutamate enhances production and galactosylation of recombinant IgG in Chinese hamster ovary cells. *Applied Microbiology and Biotechnology*, 88, 869–876.
- Amand, M. M. St., Radhakrishnan, D., Robinson, A. S., & Ogunnaike, B. A. (2014). Identification of manipulated variables for a glycosylation control strategy. *Biotechnology & Bioengineering*, 111, 1957–1970.
- Noh, S. M., Park, J. H., Lim, M. S., Kim, J. W., & Lee, G. M. (2017). Reduction of ammonia and lactate through the coupling of glutamine synthetase selection and downregulation of lactate dehydrogenase-A in CHO cells. Applied Microbiology and Biotechnology, 101, 1035–1045.
- Brodsky, A. N., Caldwell, M., Bae, S., & Harcum, S. W. (2014).
   Glycosylation-related genes in NSO cells are insensitive to moderately elevated ammonium concentrations. *Journal of Biotechnology*, 187, 78–86.
- 76. Thorens, B., & Vassalli, P. (1986). Chloroquine and ammonium chloride prevent terminal glycosylation of immunoglobulins in plasma cells without affecting secretion. *Nature*, *321*, 618–620.
- 77. Xu, X., Nagarajan, H., Lewis, N. E., Pan, S., Cai, Z., Liu, X., Chen, W., Xie, M., Wang, W., Hammond, S., Andersen, M. R., Neff, N., Passarelli, B., Koh, W., Fan, H. C., Wang, J., Gui, Y., Lee, K. H., Betenbaugh, M. J. ... Wang, J. (2011). The genomic sequence of the Chinese hamster ovary (CHO)-K1 cell line. *Nature Biotechnology*, 29, 735–741.
- Kondratova, A., Watanabe, T., Marotta, M., Cannon, M., Segall, A. M., Serre, D., & Tanaka, H. (2015). Replication fork integrity and intra-S phase checkpoint suppress gene amplification. *Nucleic acids research*, 43, 2678–2690.
- Kremkow, B. G., Baik, J. Y., MacDonald, M. L., & Lee, K. H. (2015). CHOgenome.org 2.0: Genome resources and website updates. *Biotechnology Journal*, 10, 931–938.

#### SUPPORTING INFORMATION

Additional supporting information may be found online in the Supporting Information section at the end of the article.

How to cite this article: Synoground, B. F., McGraw, C. E., Elliott, K. S., Leuze, C., Roth, J. R., Harcum, S. W., & Sandoval, N. R. (2021). Transient ammonia stress on Chinese hamster ovary (CHO) cells yield alterations to alanine metabolism and IgG glycosylation profiles. *Biotechnol J.* 16:e2100098. https://doi.org/10.1002/biot.202100098